A Mechanistic Study of the Reactions of H, O (^{3}P), and OH with Monocyclic Aromatic Hydrocarbons by Density Functional Theory

Cynthia Barckholtz, Timothy A. Barckholtz, and Christopher M. Hadad*

Department of Chemistry, The Ohio State University, 100 W. 18th Avenue, Columbus, Ohio 43210

Received: May 22, 2000; In Final Form: October 5, 2000

The chemistry of small aromatic hydrocarbons with radicals of relevance to high temperature combustion and low temperature atmospheric processes has been studied computationally using the B3LYP method and transition state theory (TST). The reaction of H, O (^{3}P), and OH with aromatic hydrocarbons can proceed by two mechanisms: hydrogen-atom abstraction or radical addition to the ring. The calculated free energies for the transition state barriers and the overall reactions show that the radical addition channel is preferred at 298 K, but the H-atom abstraction channel becomes dominant at high temperatures. The thermodynamic and kinetic preference for reactivity with aromatic hydrocarbons increases in the order O(^{3}P) < H < OH. H-atom abstraction from six-membered aromatic rings is more facile than from five-membered aromatic rings. However, radical addition to five-membered rings is thermodynamically more favorable than addition to six-membered rings. In general, the barrier heights and preferences for H-atom abstraction from sites within an aromatic hydrocarbon are well correlated with the corresponding C−H bond dissociation enthalpies.

Introduction

Elucidating the elementary reaction pathways for hydrocarbons during fuel processing and combustion is of interest not only to understand fundamental high temperature combustion chemistry, but also to gain insight into low temperature atmospheric reactions that occur following hydrocarbon emission into the environment. The chemistry of the combustion of fossil fuels such as coal and gasoline is complicated by the large fraction of aromatic compounds in the fuel. Benzene provides the simplest model with which to study the combustion of aromatic molecules. The reactions of benzene with H, O (^{3}P), and OH have been studied experimentally,[1−3] and much controversy exists over the chemistry that occurs during these reactions.

Although the reactions of benzene with H, O (^{3}P), and OH have received considerable experimental attention, very few computational studies[4] have been pursued to complement the experimental studies. Furthermore, virtually no computational studies have been undertaken to study the reactions of small radicals with heteroatomic aromatic rings. The objective of this study is to use computational methods to study the initial reactions of H, O (^{3}P), and OH with several small aromatic compounds that represent some of the functional groups known to be present in coal. Previously, it has been demonstrated[5−8] that density functional theory (DFT) methods[9,10] can be effectively applied to aromatic hydrocarbons. In this paper, the B3LYP method[11−13] was used to calculate the transition state and reaction free energies of the H-atom abstraction and radical addition pathways for furan, thiophene, pyrrole, benzene, and pyridine with H, O (^{3}P), and OH.

Free energy calculations were performed to determine the temperature dependence of the reaction pathways. However, there are very little experimental data available to compare the calculated reaction energies with experiment. Because activation barriers are not measured directly in the laboratory, it is even more difficult to evaluate the ability of the B3LYP method to accurately calculate transition state barriers. However, kinetic studies, particularly those performed over a significant temperature range, not only provide a means to determine an activation barrier, but they also provide experimental insight into the reaction mechanism as a function of temperature. Therefore, the B3LYP transition state barriers were used with nonvariational transition state theory to calculate the reaction rate constants in the temperature range 298−2000 K. Such an approach was demonstrated by Schlegel and co-workers for the study of the oxidation of methane.[14]

The focus of this paper is the elucidation of the initial reaction mechanism of several small combustion radicals with a diverse set of aromatic hydrocarbons. The preference for a particular reaction channel in the first stage of combustion chemistry has great implications for the final product channels. For example, if O atom abstracts an H atom from benzene to form the phenyl radical, subsequent oxidation and decomposition will most likely yield a cyclopentadienyl (Cp•) radical and CO_2.[15−17] However, if O atom adds to benzene, the stable adduct can undergo elimination of an H-atom to form the phenoxy radical, from which subsequent decomposition yields Cp• radical and CO as products.[18]

Further motivation for this work is to provide insight into the actual mechanism for radical addition or H-atom abstraction for the heteroatomic aromatic rings. It is difficult for experimental studies to distinguish the actual reaction center at which addition or abstraction may occur among the unique sites of an aromatic ring. This is a complicated problem for all heteroatomic aromatic rings, because it is possible that radical addition can occur at the heteroatom as well as at a ring carbon.

Finally, it is instructive to assess the validity of the B3LYP method for the calculation of thermochemical and kinetic parameters for the reactions of aromatic hydrocarbons with small radicals. A comparison between experimental studies and B3LYP calculations of reaction energies, activation barriers, rate

* Corresponding author: hadad.1@osu.edu; 614-292-1685 (fax).

10.1021/jp001884b CCC: $20.00
Published on Web 11/30/2000

constants, and temperature profiles will demonstrate which parameters can be accurately calculated by the B3LYP method for these systems.

Previous Studies

H-Atom Reactions. The simplest free radical attack on an aromatic ring is the reaction of a hydrogen atom (^{2}S) with benzene. The possible reactions that can occur include both abstraction (1) and addition (2) reactions.

$$C_6H_6 + H\bullet \rightarrow C_6H_5\bullet + H_2 \quad (1)$$

$$C_6H_6 + H\bullet \rightarrow C_6H_7\bullet \quad (2)$$

$$C_6H_7\bullet \rightarrow C_6H_6 + H\bullet \quad (3)$$

Several measurements have been made of the kinetics of reaction 1 and 2 via shock tube[19−21] and FTIR/MS[22] experiments, and for reaction 3 (the reverse of reaction 2) by radiolysis,[23−25] discharge flow tube ESR/MS,[26,27] flash photolysis-resonance fluorescence,[28] and FTIR/MS[22] experiments. The conclusion of several of these studies was that at temperatures up to 1000 K, the H (^{2}S) atom undergoes electrophilic addition to the ring to form the cyclohexadienyl radical, $C_6H_7\bullet$, instead of abstracting a hydrogen atom from a ring C−H bond.[24,26−28] However, very little effort has been made to bridge the gap between these kinetic studies and the chemistry that occurs under high temperature combustion conditions.

Recently, ab initio studies of the $C_6H_6 + H\bullet$ reaction have been performed at various levels of theory that confirmed the experimental results.[4] The activation barrier at 298 K for abstraction of an H atom from benzene to form $C_6H_5\bullet + H_2$ was calculated to be higher than that for H-atom addition to benzene. In addition, the abstraction path was determined to be an endothermic process, whereas the addition of H atom to C_6H_6 to form $C_6H_7\bullet$ was calculated to be exothermic.

O (^{3}P) Atom Reactions. More controversy exists over the preferred pathway for the reaction of an oxygen atom with benzene than for the reaction of benzene with a hydrogen atom. The addition of atomic oxygen to benzene occurs by formation of a long-lived triplet biradical.[29]

$$C_6H_6 + O\ (^3P) \rightarrow C_6H_6O \quad (4)$$

Alternatively, hydrogen abstraction by an oxygen atom can occur to produce phenyl and hydroxyl radicals.

$$C_6H_6 + O\ (^3P) \rightarrow C_6H_5\bullet + \bullet OH \quad (5)$$

A few kinetic measurements of the reaction of oxygen atoms with benzene have been reported,[30−36] but very few experiments have been able to elucidate the mechanism for this reaction.[29,31,32,37] Most studies (T < 1000 K) have concluded that the reaction of oxygen atom with benzene proceeds via addition to the ring.[29,31,32] However, OH formation has been observed[37] in crossed-beam experiments at high collision energies that correspond to a temperature high enough to overcome the endothermicity of reaction 5.

OH Radical Reactions. A relatively large number of kinetic studies have been reported for the reaction of the hydroxyl radical with benzene, and the results of these studies are summarized as part of lengthy reviews on the chemistry of hydroxyl radicals under atmospheric conditions.[1,38,39] The prevalent view is that two reaction channels for the reaction of OH with benzene are available that dominate in different temperature regimes. The first is the electrophilic addition to the benzene ring[40] to form the hydroxycyclohexadienyl radical that can be collisionally stabilized but will decompose back to reactants at moderate temperatures ($T \geq$ 325 K).[41−43]

$$C_6H_6 + \bullet OH \rightleftharpoons C_6H_6OH\bullet \quad (6)$$

The abstraction channel is thought to be a minor channel at low temperatures and only becomes significant at temperatures greater than 600 K.[41,42,44]

$$C_6H_6 + \bullet OH \rightarrow C_6H_5\bullet + H_2O \quad (7)$$

However, the preference for abstraction at high temperatures has been questioned in favor of an addition−elimination path that generates phenol.[45]

$$C_6H_6 + \bullet OH \rightarrow C_6H_6OH\bullet \rightarrow C_6H_5OH + H\bullet \quad (8)$$

The uncertainty in the reaction products warrants further study of the attack of hydroxyl radical on benzene.

Heteroatomic Aromatic Hydrocarbon Reactions. The additional functional groups present in the aromatic network of coal add greater complexity to the reactions with H, ^{3}O, and OH that occur during coal combustion. However, there have been few studies of the reactions of heteroatomic aromatic hydrocarbons with H, O (^{3}P), and OH reported in the literature. A kinetic measurement of the reaction of O (^{3}P) with pyridine[35] determined that the addition reaction occurred with a lower activation barrier than for the analogous reaction with benzene. Furthermore, it was deduced from the observed product distribution that there was a preference for electrophilic addition to pyridine at the meta position.

There are also a few reports of the reactions of O (^{3}P) with five-membered aromatic rings such as furan,[46] thiophene,[46−48] and pyrrole.[46] Although there is disagreement in the kinetic results from these experiments, evidence was found solely for addition to the aromatic ring for T < 525 K. Reactivity studies of the five-membered aromatic rings, furan and pyrrole, with H and OH in aqueous solution indicate that addition of these radicals occurs at the ortho position.[49,50]

Similar investigations of the reaction of hydroxyl radical with five-membered aromatic rings have been performed to determine the available reaction channels. There is general agreement that the reaction of OH with furan proceeds via addition to a carbon−carbon double bond,[51,52] analogous to the reaction of oxygen atoms with furan.[46] It was also proposed that addition at the ortho position in furan would be preferred over addition at the meta position due to the existence of an additional resonance structure in the addition product.[53,54] Addition is also thought to be the preferred mechanism for the reaction of the hydroxyl radical with thiophene. Most experiments to date have been inconclusive about the actual addition mechanism.[51,52,55] However, the barrier height for the reaction of OH with thiophene is thought to be lower than that for furan, based on the recommended Arrhenius rate expression for these five-membered aromatic rings.[1]

Computational Methods

The potential energy surfaces for the reactions of H, O, and OH with monocyclic aromatic hydrocarbons were studied using DFT.[9,10] All geometry optimizations and frequency calculations were performed using Gaussian 94[56] at the Ohio Supercomputer Center. The geometry of each structure was fully optimized at

the B3LYP/6-31G(d) level.[11−13] Transition structures and products of aromatic hydrocarbons reactions with H and OH were treated as doublets. Corresponding structures for the reactions with O atom were calculated as the triplet spin state. Harmonic vibrational frequencies have also been calculated for each stationary point to verify the correct number of real and imaginary frequencies and to provide zero-point vibrational energy (ZPE) corrections, which were scaled by a factor of 0.9806.[57] The thermodynamic contributions to the enthalpy and free energy were also obtained from the unscaled vibrational frequencies in order to calculate $\Delta H(T)$ and $\Delta G(T)$, respectively. Transition states were confirmed to connect to reactants and products by incremental displacement (typically 10%) of the structure of the transition state along the normal mode for the imaginary vibrational frequency in each direction, followed by calculation of the analytical force constants and subsequent optimization (opt = calcfc). Intrinsic reaction coordinate (IRC) searches[58,59] were also used in some cases.

In our recent study of aromatic hydrocarbons,[5] it was shown that the B3LYP/6-31G(d) level of theory can be used to reliably calculate C−H bond dissociation enthalpies (BDE), and expansion of the basis set to 6-311+G(d,p) led to an improvement in the calculated dissociation enthalpy for the more polar N−H bond. Another recent study[60] showed that the B3LYP method could be used to calculate the potential energy surface (PES) of the thermal decomposition of pyrrole in good agreement with the more computationally demanding G2(MP2) method. Bauschlicher and Langhoff showed recently that B3LYP/4-31G calculations yield reasonable BDEs, but larger basis sets were necessary for reactions involving electronegative heteroatoms.[8] Therefore, single point energies at the B3LYP/6-311+G(d,p)//B3LYP/6-31G(d) level, using six Cartesian *d* functions, were calculated in order to obtain more reliable energies for the PES.

Spin contamination, while a significant problem for unrestricted Hartree−Fock (UHF) wave functions for these species, is not a significant issue for the B3LYP wave functions.[61] The $\langle S^2 \rangle$ value for doublet species calculated by the UB3LYP method for the aryl radicals ranged from a typical value of ~0.76 to a maximum value of ~0.79. Conversely, UCCSD(T) and UQCISD(T) calculations with a 6-31+G(d,p) basis set (for the H-atom abstraction transition states and products with furan) were unsuccessful due to a lack of convergence at the SCF level or in the coupled cluster iterations. Spin contamination is a possible issue in the application of the CBS-QB3[62] method to these aromatic systems, although CBS-QB3 enthalpies for benzene, the phenyl radical, the radicals H, O, and OH, and their respective parent species prior to H-atom abstraction were calculated using Gaussian 98.[63] Spin contamination also causes great difficulty in applying UCCSD(T) and/or UQCISD(T) methods for these systems. While others have utilized restricted open shell CCSD methods,[64−67] the lack of size consistency is of concern in a comparison over a diverse class of molecules and reaction pathways. During the review process for this manuscript, we became aware of a recent study by Truhlar and co-workers. We then also applied their MPW1K method[68] to a limited subset of the reactions considered here.

The B3LYP/6-311+G(d,p)//B3LYP/6-31G(d) transition state energies were used with nonvariational transition state theory with a Wigner estimate for the tunneling correction, $\Gamma(T)$ to calculate reaction rate constants[69]

$$k(T) = \Gamma(T)\frac{k_B T}{Nh}\frac{Q_{TS}^{\ddagger}(T)}{Q_{Ar}(T)Q_X(T)}e^{-E_0/RT} \tag{9}$$

with

$$\Gamma(T) = 1 + \frac{1}{24}\left(\frac{h\nu_i}{k_B T}\right)^2 \tag{10}$$

where $Q_{TS}^{\ddagger}(T)$, $Q_{Ar}(T)$, and $Q_X(T)$ are the total partition functions for the transition state, the aromatic hydrocarbon, and X = H, O, or OH, respectively, at temperature T, k_B is the Boltzmann constant, h is Planck's constant, and ν_i is the imaginary vibrational frequency of the transition state. For O and OH, the electronic partition function was calculated using the experimental splittings for the low-lying excited states.[70,71] Using eq 9, calculated rate constants can be directly compared to experimental rate constants.

The temperature dependence of these reactions were also studied. The experimental activation energy, E_a, is defined by the equation

$$\frac{d \ln k}{dT} \equiv \frac{E_a}{RT^2} \tag{11}$$

For a reaction that obeys the Arrhenius equation,

$$k(T) = Ae^{-E_a/RT} \tag{12}$$

a plot of ln k vs $1/T$ yields a slope that is equal to $-E_a/R$ and the computed activation barrier can be compared directly to an experimental Arrhenius activation barrier. Rate constants were computed over the temperature range 298−2000 K and then fitted to the Arrhenius equation to determine E_a and A. A recent paper[72] has shown that DFT methods can be used to reliably calculate the preexponential, A, factor as well as reproduce the Arrhenius plot curvature for hydrogen-abstraction reactions.

A curved Arrhenius plot results when E_a is dependent on temperature. Therefore, reaction rate constants were also fit by the equation

$$k(T) = AT^m e^{-E_{0K}/RT} \tag{13}$$

A plot of $\ln(k/T^m)$ vs $1/T$ yields a slope that is equal to E_{0K}/R where E_{0K} is the hypotheical activation barrier at absolute zero and is related to E_a by the equation

$$E_a = E_{0K} + mRT \tag{14}$$

Although the B3LYP method has been shown to perform well in the calculation of geometries, vibrational frequencies, and reaction energies, one criticism of the technique is that it fails to accurately predict transition state barriers. Although some computational studies[73,74] have shown that the B3LYP method consistently underestimates (by ~4−6 kcal mol^{-1}) the activation energies calculated at other correlated levels, other studies[75,76] indicate that B3LYP activation energies are in good (within 2 kcal mol^{-1}) agreement with experimental activation energies for H-atom abstraction reactions. Therefore, it would appear that the accuracy of the B3LYP method for the calculation of activation barriers should be judged separately for different reaction systems. Furthermore, since a general knowledge of the reaction of H, O, and OH with aromatic hydrocarbons relevant to coal combustion is sought, a comparison of the $k_{add}/k_{abstract}$ ratio as a function of temperature will minimize any effect of a systematic error in the B3LYP calculation of transition state barriers.

Computational Results

Two reaction channels — radical addition and H-atom abstraction — were explored for the initial step in the oxidation

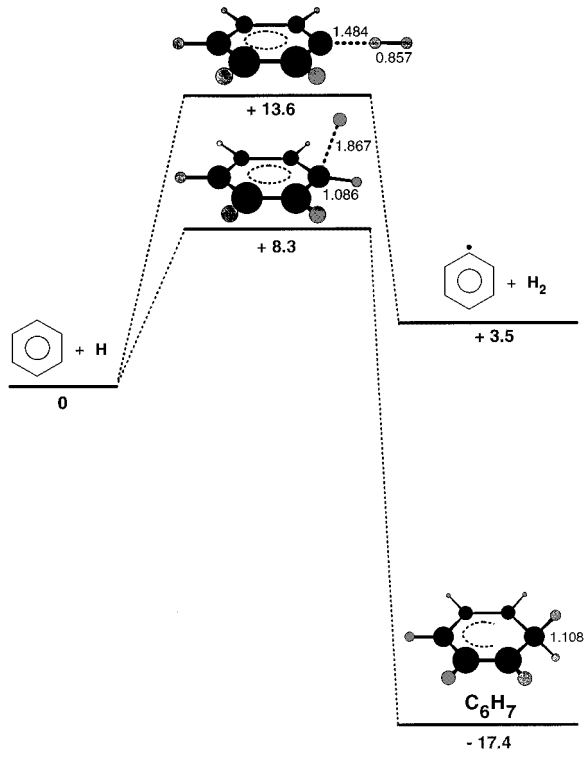

Figure 1. Profile of the free energy surface for the reaction of C_6H_6 + H at 298 K, calculated at the B3LYP/6-311+G(d,p)//B3LYP/6-31G-(d) level of theory (in kcal mol^{-1}).

of benzene, pyridine, furan, thiophene, and pyrrole. Although the thermochemistry and kinetics for the reaction of benzene with H atoms has been studied previously,[4] the analogous reactions with other combustion radicals or other aromatic hydrocarbons have not been addressed by computational methods. Here, the reactant and product minima, and the transition states that connect them, for more than 80 unique reactions of H, O (^{3}P), and OH with aromatic hydrocarbons have been studied using the B3LYP method.

Reactions of Hydrogen Atoms with Benzene. The reaction of benzene with H atom was studied along both the H-atom addition channel to form C_6H_7• and the H-atom abstraction channel to form C_6H_5• + H_2 (Figure 1 and Table 1). At 298 K, the addition channel has a modest transition state free energy ($\Delta G^{\ddagger}$) of 8.3 kcal mol^{-1} and is exoergic by 17.4 kcal mol^{-1}. In contrast, the abstraction channel has a higher $\Delta G^{\ddagger}$ (13.6 kcal mol^{-1}) and is endoergic by 3.5 kcal mol^{-1}. The B3LYP transition state and reaction free energy presented here for the addition pathway are in good agreement with the high level calculations of Lin, Morokuma, and co-workers[4] (though their calculations only included ZPE corrections, and were not full free energy calculations). However, the H-atom abstraction pathway results are not in as good agreement with the higher level QCISD(T) and G2M(rcc,MP2) levels due to the apparent underestimation of both the transition state and product energies by the B3LYP method.

A better test for the B3LYP method is to compare the calculations with experiment. A direct comparison of transition state and reaction free energies between theory and experiment is not available. However, calculation of the thermochemical and kinetic parameters throughout a temperature range facilitates the comparison. Energetically, the H-atom abstraction channel from benzene is calculated to be kinetically favored over H-atom addition to benzene at temperatures above ~1155 K. This result supports the experimental determination that the abstraction channel is negligible at temperatures less than 1000 K.[28]

Sauer and co-workers have studied the addition channel by following the UV absorption of the cyclohexadienyl (C_6H_7•) radical. In separate experiments,[23,24] they determined the activation energy for the addition of H atom to benzene to be 3.3 and 4.3 kcal mol^{-1}. These values are in good agreement with the fitted (T = 298−2000 K) B3LYP-TST E_a of 3.2 kcal mol^{-1} (Table 1). It should be noted that the G2M(rcc,MP2) calculations of Lin, Morokuma, and co-workers determined an $E_0^{\ddagger}$ of 8.9

TABLE 1: Thermodynamic and Kinetic Parameters for the Reaction of Monocyclic Aromatic Hydrocarbons with H Atom for the H-atom Abstraction Channel (a) and Radical Addition Channel (b)[a]

molecule	site	$E_{0,rxn}$	ΔH_{rxn}	ΔG_{rxn}	$E_0^{\ddagger}$	$\Delta H^{\ddagger}$	$\Delta G^{\ddagger}$	ln $k_{forward}$	E_a	m	E_{0K}
(a) H-Atom Abstraction by H Atom											
benzene	1	5.53	5.99	3.46	10.00	9.61	13.64	−40.82	10.43 ± 0.40	1.08 ± 0.06	9.05 ± 0.08
pyridine	2	−0.23	0.36	−1.52	7.92	7.07	13.25	−39.90	7.52 ± 0.38	0.94 ± 0.05	6.32 ± 0.06
	3	5.84	6.42	4.54	11.42	10.64	16.66	−45.91	11.28 ± 0.37	0.90 ± 0.02	10.13 ± 0.03
	4	4.55	5.13	3.67	10.69	9.89	16.36	−45.35	10.50 ± 0.37	0.94 ± 0.02	9.30 ± 0.02
furan	2	13.45	14.06	12.14	17.36	16.73	22.34	−55.73	17.57 ± 0.36	0.88 ± 0.05	16.45 ± 0.07
	3	13.21	13.79	11.92	16.82	16.15	21.86	−54.95	16.99 ± 0.35	0.83 ± 0.06	15.92 ± 0.08
thiophene	2	11.40	12.03	10.05	15.25	14.59	20.29	−52.27	15.41 ± 0.35	0.83 ± 0.05	14.34 ± 0.07
	3	8.53	9.13	7.21	13.18	12.44	18.35	−48.88	13.16 ± 0.36	0.85 ± 0.04	12.07 ± 0.06
pyrrole	2	12.90	13.65	11.46	16.75	16.21	21.59	−54.48	17.09 ± 0.36	0.89 ± 0.08	15.95 ± 0.10
	3	12.43	13.05	11.12	16.17	15.51	21.21	−53.84	16.33 ± 0.35	0.82 ± 0.04	15.29 ± 0.05
	N	−12.08	−11.54	−12.95	22.05	21.10	27.78	−64.96	21.60 ± 0.26	0.46 ± 0.07	21.02 ± 0.09
(b) H−Atom Addition											
benzene	1	−22.23	−23.30	−17.42	3.77	2.73	8.28	−31.91	3.22 ± 0.29	0.55 ± 0.01	2.52 ± 0.01
pyridine	2	−22.61	−23.66	−17.20	4.18	3.13	9.75	−34.36	3.61 ± 0.29	0.55 ± 0.02	2.90 ± 0.03
	3	−23.05	−24.08	−17.69	4.01	2.97	9.58	−34.08	3.47 ± 0.29	0.56 ± 0.01	2.75 ± 0.01
	4	−22.09	−23.20	−16.16	4.41	3.36	9.98	−34.74	3.83 ± 0.29	0.57 ± 0.02	3.11 ± 0.02
furan	2	−33.54	−34.62	−28.03	1.38	0.44	6.83	−29.75	1.15 ± 0.27	0.49 ± 0.01	0.53 ± 0.01
	3	−21.34	−22.43	−15.82	3.91	2.83	9.50	−33.96	3.29 ± 0.28	0.52 ± 0.02	2.63 ± 0.03
thiophene	2	−34.98	−36.04	−29.52	2.11	1.13	7.61	−30.96	1.76 ± 0.28	0.52 ± 0.01	1.10 ± 0.01
	3	−23.51	−24.29	−18.50	3.39	2.35	8.95	−33.08	2.87 ± 0.28	0.53 ± 0.02	2.19 ± 0.03
pyrrole	2	−27.20	−28.35	−21.64	0.85	−0.12	6.32	−28.92	0.59 ± 0.26	0.45 ± 0.02	0.01 ± 0.03
	3	−18.24	−19.33	−12.72	3.27	2.18	8.86	−32.90	2.63 ± 0.27	0.50 ± 0.02	1.99 ± 0.03
	N	15.82	14.74	21.35	17.98	16.68	23.67	−57.19	16.41 ± 0.21	0.28 ± 0.19	16.06 ± 0.25

[a] B3LYP/6-311+G(d,p)//B3LYP/6-31G(d) reaction (rxn) and transition state (‡) energies are reported relative to reactants, in kcal mol^{-1}. E_0 energies include scaled ZPE. ΔH_{rxn}, ΔG_{rxn}, and ln $k_{forward}$ are given at 298.15 K. E_a values are obtained from a fit of ln k vs $1/T$ (see eq 12) where T = 298−2000 K. m and E_{0K} are obtained from fits of ln(k/T^m) vs $1/T$ (see eq 13) where T = 298−2000 K.

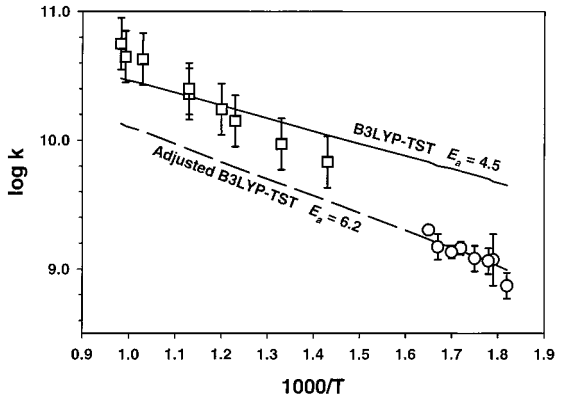

Figure 2. Arrhenius plot of the rate constant for the $C_6H_5 + H_2$ reaction ($T = 550-1025$ K). Experimental data shown by ○ are k data ($T = 550-650$ K) taken directly from ref 22 (error bars from ref 22). Experimental data shown by □ are log k ($T = 700-1017$ K) extracted from Fig. 5 in ref 22 (error bars assigned based on 50% error in k data). A fit to the experimental data shown gives $E_a = 9.7$ kcal mol^{-1}. The calculated results using B3LYP-TST with Arrhenius parameters fitted from $T = 298-2000$ K (eq 12) are shown by the straight lines with 1.7 kcal mol^{-1} added to E_a to give the "adjusted" B3LYP-TST line.

kcal mol^{-1} for this reaction.[4] Therefore, one would expect the experimental E_a to be higher, differing only by ~2 kcal mol^{-1} from the $E_0^{\ddagger}$ value[68] if pressure and tunneling effects were negligible.

To explore the quality of the calculation for the H-atom abstraction channel, the B3LYP results for the abstraction pathway were compared to the experimental rate constant by Lin and co-workers.[22] An Arrhenius fit to the rate constant for the $C_6H_5\bullet + H_2$ reaction from ref 22 gives an E_a of ~9.7 kcal mol^{-1}. Previous theoretical calculations at the G2M(rcc,MP2) level obtained an $E_0^{\ddagger}$ of 8.8 kcal mol^{-1},[4] in good agreement with experiment. For a direct comparison of the B3LYP-TST method, the energetic parameters for the reverse abstraction reaction, $C_6H_5\bullet + H_2$, were calculated over the temperature range of 298−2000 K. An Arrhenius fit ($T = 298-2000$ K) to the B3LYP energies gives an activation barrier of 4.5 kcal mol^{-1}. The calculated B3LYP rate constants are too fast compared to the lower temperature ($T \approx 550-650$ K) experimental $C_6H_5\bullet + H_2$ rate constants. Similar attempts[68] to calculate barrier heights have shown that very often a small adjustment of the calculated barrier will bring the calculated and experimental rate constants into close agreement. Following this reasoning, if one were to add 1.7 kcal·mol^{-1} to the B3LYP calculated barrier, then the agreement with the lower temperature experimental data is excellent (Figure 2), although the agreement with the higher temperature data ($T \approx 700-1000$ K) is less good. The similarity of the B3LYP-TST and experimental *y*-intercept values (i.e., log *k*) suggests that the B3LYP-TST method calculates a preexponential factor, *A*, that is in reasonably good agreement with experiment for this reaction. However, better agreement with the experimental rate constants may be obtained with improvement in the level of transition state theory used with the B3LYP potential energy surfaces. However, we believe that qualitative comparison of the different aromatic reaction pathways can still be made.

Reactions of Hydrogen Atom with Heteroatomic Aromatic Hydrocarbons. The H-atom addition and abstraction channels were also explored for the reactions of pyridine, furan, thiophene, and pyrrole (Table 1). Analogous to the reaction with benzene, the H-atom addition reaction is exoergic at 298 K for all of these heteroatomic aromatic hydrocarbons. The transition state free energy for the addition of H atom to pyridine is approximately the same at all three unique ring carbon positions and is just slightly higher than that for H-atom addition to benzene. The lowest barrier for H-atom addition to pyridine, 9.6 kcal mol^{-1}, is for addition to the meta carbon.

TABLE 2: A Comparison of $k_{add}/k_{abstract}$ as a Function of Temperature for the Reaction of Aromatic Hydrocarbons with H Atom[a]

		298 K	500 K	1000 K	1500 K	2000 K
benzene		7318	66	1.7	0.45	0.23
pyridine	2	254	20	2.8	1.3	0.9
	3	1.4×10^5	754	15	3.7	1.8
	4	4.1×10^4	493	17	5.1	2.7
furan	2	1.9×10^{11}	3.1×10^6	765	45	11
	3	1.3×10^9	1.3×10^5	129	12	3.7
thiophene	2	2.5×10^8	5.7×10^4	103	12	4.0
	3	7.3×10^6	7.4×10^3	41	6.8	2.7
pyrrole	2	1.3×10^{11}	2.0×10^6	465	27	6.4
	3	1.2×10^9	1.2×10^5	121	11	3.5

[a] Rate constants were calculated using eq 9 based on the B3LYP/6-311+G(d,p)//B3LYP/6-31G(d) level of theory.

While the H-atom abstraction reaction is endoergic at the meta and para carbons of pyridine, abstraction from the ortho carbon is 1.5 kcal mol^{-1} exoergic. Also, the computed transition state free energy for H-atom abstraction from the ortho carbon of pyridine, 13.3 kcal mol^{-1}, is ~3 kcal mol^{-1} lower than the barrier for abstraction from the other C−H ring positions in pyridine.

The free energy surfaces for the reactions of H atom with the five-membered aromatic rings are qualitatively similar to those for the reaction of H atom with either benzene or pyridine: the addition pathway is thermodynamically preferred over the H-atom abstraction pathway. However, the surfaces are quite different quantitatively. For simplicity, only furan will be discussed in detail as it is representative of the chemistry of the five-membered ring compounds. The transition state barrier for H-atom addition to furan is ~3 kcal mol^{-1} lower at the ortho position than at the meta position. Also, for the overall reaction free energy at 298 K, it is >12 kcal mol^{-1} more favorable for the H atom to add to the ortho carbon of furan rather than the meta carbon.

The very large barriers (~22 kcal mol^{-1}) for H-atom abstraction from the five-membered aromatic rings gives rise to room-temperature reaction rates that are $\sim 10^9$ times slower than the H-atom addition channel (Table 2). At elevated temperatures; however, the H-atom abstraction channel can compete with the addition channel. Throughout the temperature range of 298−2000 K, there is a slight preference, more evident in thiophene than in furan or pyrrole, for H-atom abstraction from the 3 position over the 2 position.

A comparison of the ratio of the calculated rate constants for the addition channel with respect to the abstraction channel ($k_{add}/k_{abstract}$) for the five- and six-membered aromatic rings is shown in Table 2. It is evident that the five-membered rings (furan, thiophene, and pyrrole) will be less susceptible to H-atom abstraction throughout a larger temperature range than will the six-membered rings (benzene and pyridine). Furthermore, H-atom abstraction from the five-membered rings should not be favorable even at the highest temperature studied here (2000 K). In contrast, the H-atom abstraction channel will be competitive with H-atom addition at temperatures greater than 1000 and 1500 K for the six-membered rings benzene and pyridine, respectively.

Reactions of Oxygen Atom with Benzene. The PES for the initial reaction of benzene with O atoms was studied by the

TABLE 3: Thermodynamic and Kinetic Parameters for the Reaction of Monocyclic Aromatic Hydrocarbons with O Atom for the H-atom Abstraction Channel (a) and Radical Addition Channel (b)[a]

molecule	site	$E_{0,rxn}$	ΔH_{rxn}	ΔG_{rxn}	$E_0^{\ddagger}$	$\Delta H^{\ddagger}$	$\Delta G^{\ddagger}$	ln $k_{forward}$	E_a	m	E_{0K}
H-Atom Abstraction by O Atom											
benzene	1	7.51	7.86	4.97	4.49	4.09	10.10	−35.16	5.51 ± 0.48	1.53 ± 0.13	3.56 ± 0.17
pyridine	2	1.77	2.23	−0.01	0.95	0.50	7.70	−30.43	1.42 ± 0.49	1.58 ± 0.11	−0.59 ± 0.14
	3	7.83	8.29	6.05	5.44	5.00	11.97	−38.35	6.40 ± 0.47	1.47 ± 0.13	4.52 ± 0.17
	4	6.55	7.00	5.19	4.28	4.37	9.44	−34.28	5.93 ± 0.43	1.21 ± 0.22	4.39 ± 0.29
furan	2	15.45	15.93	13.65	13.76	13.68	19.72	−51.65	15.22 ± 0.43	1.23 ± 0.16	13.66 ± 0.21
	3	15.20	15.66	13.43	13.43	13.23	19.55	−51.38	14.69 ± 0.40	1.09 ± 0.14	13.30 ± 0.19
thiophene	2	13.40	13.90	11.57	13.53	13.33	19.83	−51.83	14.78 ± 0.42	1.15 ± 0.13	13.31 ± 0.17
	3	10.52	11.00	8.73	9.07	8.70	15.40	−44.30	10.13 ± 0.44	1.26 ± 0.10	8.52 ± 0.13
pyrrole	2	14.90	15.52	12.97	11.35	10.87	17.87	−48.48	12.23 ± 0.42	1.19 ± 0.07	10.71 ± 0.10
	3[b]	14.43	8.29	6.05							
	N[b]	−10.08	7.00	5.19							
(b) O−Atom Addition											
benzene	1	−9.46	−10.25	−3.06	0.01	−0.71	6.36	−28.94	0.21 ± 0.33	0.71 ± 0.05	−0.70 ± 0.07
pyridine	2	−16.41	−17.14	−8.93	2.54	1.79	9.94	−35.00	2.67 ± 0.31	0.65 ± 0.04	1.84 ± 0.06
	3	−16.14	−16.81	−8.70	0.52	−0.18	7.83	−31.46	0.74 ± 0.32	0.67 ± 0.04	−0.12 ± 0.05
	4	−12.76	−13.51	−5.18	2.45	1.71	9.91	−34.93	2.59 ± 0.32	0.69 ± 0.05	1.71 ± 0.07
furan	2[c]	−34.09	−34.85	−26.51							
	3	−14.36	−15.09	−6.82	−1.69	−2.43	5.62	−27.70	−1.57 ± 0.31	0.64 ± 0.02	−2.38 ± 0.02
thiophene	2	−28.33	−28.93	−20.87	−4.28	−4.98	2.95	−23.30	−4.08 ± 0.29	0.55 ± 0.02	−4.78 ± 0.02
	3	−16.23	−16.85	−8.79	−1.63	−2.35	5.69	−27.85	−1.48 ± 0.30	0.61 ± 0.04	−2.26 ± 0.06
pyrrole	2[c]	−26.99	−27.78	−19.41							
	3	−13.55	−14.05	−6.27	−3.10	−3.86	4.26	−25.41	−3.00 ± 0.31	0.63 ± 0.03	−3.80 ± 0.05
	N	29.46	28.67	37.12	29.40	28.56	37.05	−80.39	29.28 ± 0.36	0.86 ± 0.07	28.17 ± 0.10

[a] B3LYP/6-311+G(d,p)//B3LYP/6-31G(d) reaction (rxn) and transition state (‡) energies are reported relative to reactants, in kcal mol^{-1}. E_0 energies include scaled ZPE. ΔH_{rxn}, ΔG_{rxn}, and ln $k_{forward}$ are given at 298.15 K. E_a values are obtained from a fit of ln k vs $1/T$ (see eq 12) where T = 298−2000 K. m and E_{0K} are obtained from fits of ln(k/T^m) vs $1/T$ (see eq 13) where T = 298−2000 K. [b] The transition structure was not located for these reactions. [c] Barrierless reaction.

TABLE 4: Comparison of $k_{add}/k_{abstract}$ as a Function of Temperature for the Reaction of Aromatic Hydrocarbons with O Atom[a,b]

		298 K	500 K	1000 K	1500 K	2000 K
benzene		503	18	1.2	0.42	0.24
pyridine	2	0.010	0.034	0.060	0.061	0.059
	3	988	28	1.5	0.51	0.28
	4	0.53	0.067	0.012	0.0061	0.0043
furan	3	1.9×10^{10}	3.6×10^{5}	95	6	1.4
thiophene	2	2.5×10^{12}	8.2×10^{6}	582	22	4.1
	3	1.4×10^{7}	6540	18	2.3	0.77

[a] $k_{add}/k_{abstract}$ ratios were not calculated for furan at the 2 position and pyrrole at the 2 and 3 positions due to the lack of a transition state barrier for either the O-atom addition or H-atom abstraction channel. [b] Rate constants were calculated using eq 9 based on the B3LYP/6-311+G(d,p)//B3LYP/6-31G(d) level of theory.

B3LYP method (Table 3). The product of the addition channel is a triplet biradical C_6H_6O. (Subsequent reactions of this biradical will be presented elsewhere.) At 298 K, the addition channel has a modest $\Delta G^{\ddagger}$ (6.4 kcal mol^{-1}) and is exoergic by 3.1 kcal mol^{-1}. The B3LYP calculations show that the addition channel for the reaction of atomic oxygen with benzene is preferred over H-atom abstraction at room temperature, in agreement with earlier experimental studies.[29,31,32]

The abstraction channel, leading to the formation of $C_6H_5\bullet$ + OH, has a $\Delta G^{\ddagger}$ = 10.1 kcal mol^{-1}, and the reaction is endoergic by 5.0 kcal mol^{-1} at 298 K. The entropy contributions will favor the H-atom abstraction channel at elevated temperatures. Even so, experimental kinetic studies at temperatures up to 950 K have shown no evidence for the formation of OH as a product.[31] In agreement with these observations, the B3LYP calculations find that the transition state free energy for H-atom abstraction from benzene becomes lower than that for addition at ~1065 K. A comparison of the $k_{add}/k_{abstract}$ ratio from the B3LYP rate constant calculations (Table 4) is also in agreement with the experimental observation that OH formation from the reaction of atomic oxygen with benzene[37] occurs only at high collision energies, i.e., "high temperatures."

An absolute comparison of the B3LYP kinetic parameters (T = 298−2000 K) for the addition reaction C_6H_6 + O (^{3}P) → C_6H_6O (E_a = 0.21 kcal mol^{-1}) with experiment (E_a = 4.0,[33,36] 4.8,[31] and 5.0[32] kcal mol^{-1}) illustrates the deficiencies in the calculation. The B3LYP Arrhenius plot (ln k vs $1/T$) does show significant curvature, indicating E_a is not constant over this temperature range. Also, at 298 K, the rate constant for O-atom addition is calculated to be an order of magnitude too slow with respect to one experimental study[31] and an order of magnitude too fast with respect to earlier experimental studies.[33,36] Therefore, a comparison of the B3LYP-TST kinetic parameters with experimental parameters is ill-defined, since the scatter in the experimental rate constants (and preexponential factors) is fairly large despite the agreement in activation energy.

Reactions of Oxygen Atom with Heteroatomic Aromatic Hydrocarbons. The potential energy surfaces for the reactions of O atoms with pyridine, furan, thiophene, and pyrrole (Table 3) are qualitatively similar to the analogous H-atom reactions. Although the $\Delta G^{\ddagger}$ for addition of O atom to each of the 3 unique ring carbons of pyridine is a few kcal mol^{-1} higher than for O-atom addition to benzene, the overall reaction free energy is several kcal mol^{-1} more exoergic. The H-atom abstraction channel is as favorable as the addition channel for the room-temperature reaction of pyridine with O atom. The most favored sites from which H-atom abstraction will occur are the ortho and para C−H bonds of pyridine. Furthermore, the calculations support the experimental observation[35] that O-atom addition to pyridine is considerably favored at the meta position.

In contrast to the six-membered rings, the $\Delta G^{\ddagger}$ for O-atom addition to the five-membered rings is either lower in energy or barrierless. The B3LYP calculations suggest that transition state structures do not exist for several of the addition products. For example, there is an asymptotic energy profile for the

TABLE 5: Thermodynamic and Kinetic Parameters for the Reaction of Monocyclic Aromatic Hydrocarbons with OH Radical for the H-atom Abstraction Channel (a) and Radical Addition Channel (b)[a]

molecule	site	$E_{0,rxn}$	ΔH_{rxn}	ΔG_{rxn}	$E_0^{\ddagger}$	$\Delta H^{\ddagger}$	$\Delta G^{\ddagger}$	ln $k_{forward}$	E_a	m	E_{0K}
					(a) H−Atom Abstraction by OH						
benzene	1	−4.62	−4.33	−5.92	0.35	−0.12	7.20	−29.43	0.90 ± 0.57	2.19 ± 0.02	−1.91 ± 0.07
pyridine	2	−10.25	−9.96	−10.90	−2.68	−3.15	5.13	−26.12	−2.05 ± 0.57	2.15 ± 0.02	−4.80 ± 0.05
	3	−4.19	−3.90	−4.84	0.49	0.02	8.35	−31.37	1.03 ± 0.57	2.19 ± 0.03	−1.77 ± 0.08
	4	−5.48	−5.19	−5.70	0.22	−0.25	8.09	−30.93	0.77 ± 0.58	2.22 ± 0.03	−2.06 ± 0.07
furan	2	3.42	3.74	2.76	5.60	5.22	13.13	−39.66	6.39 ± 0.57	2.18 ± 0.02	3.61 ± 0.04
	3	3.18	3.47	2.54	4.85	4.40	12.62	−38.73	5.51 ± 0.57	2.17 ± 0.02	2.73 ± 0.05
thiophene	2	1.37	1.71	0.68	3.82	3.44	11.49	−36.79	4.51 ± 0.57	2.16 ± 0.02	1.76 ± 0.05
	3	−1.50	−1.19	−2.16	2.17	1.72	10.03	−34.20	2.72 ± 0.57	2.17 ± 0.03	−0.05 ± 0.07
pyrrole	2	2.87	3.33	2.08	3.64	3.09	11.50	−36.90	4.09 ± 0.55	2.03 ± 0.03	1.50 ± 0.09
	3	2.41	2.73	1.75	3.66	3.19	11.49	−36.78	4.25 ± 0.57	2.15 ± 0.02	1.51 ± 0.06
	N[b]	−22.10	−21.86	−22.32							
					(b) OH Addition						
benzene	1	−13.15	−14.15	−5.26	−0.73	−1.51	6.73	−29.65	−0.30 ± 0.45	1.37 ± 0.03	−2.05 ± 0.08
pyridine	2	−15.79	−16.74	−6.95	1.68	0.91	10.22	−35.52	2.11 ± 0.46	1.39 ± 0.03	0.34 ± 0.07
	3	−13.11	−14.07	−4.25	−0.32	−1.10	8.18	−32.10	0.13 ± 0.46	1.39 ± 0.03	−1.65 ± 0.07
	4	−11.10	−12.11	−2.12	1.55	0.78	10.04	−35.21	1.98 ± 0.46	1.41 ± 0.03	0.18 ± 0.07
furan	2[c]	−30.99	−32.09	−21.93							
	3	−13.40	−14.28	−4.57	−1.80	−2.66	6.78	−29.72	−1.50 ± 0.45	1.34 ± 0.03	−3.21 ± 0.09
thiophene	2	−27.05	−28.07	−18.06	−3.98	−4.69	4.33	−25.69	−3.40 ± 0.45	1.35 ± 0.03	−5.13 ± 0.08
	3	−14.64	−15.54	−5.79	−1.80	−2.60	6.71	−29.63	−1.40 ± 0.45	1.34 ± 0.03	−3.11 ± 0.09
pyrrole	2[c]	−24.18	−25.28	−15.13							
	3	−11.73	−12.60	−2.88	−2.91	−3.79	5.70	−27.90	−2.64 ± 0.44	1.32 ± 0.04	−4.33 ± 0.10
	N[d]										

[a] B3LYP/6-311+G(d,p)//B3LYP/6-31G(d) reaction (rxn) and transition state (‡) energies are reported relative to reactants, in kcal·mol^{-1}. E_0 energies include scaled ZPE. ΔH_{rxn}, ΔG_{rxn}, and ln $k_{forward}$ are given at 298.15 K. E_a values are obtained from a fit of ln k vs $1/T$ (see eq 12) where $T = 298-2000$ K. m and E_{0K} are obtained from fits of ln(k/T^m) vs $1/T$ (see eq 13) where $T = 298-2000$ K. [b] The transition structure was not located for these reactions. [c] Barrierless reaction. [d] Transition state and product do not exist for this reaction.

addition channel (i.e., a barrierless process) for the addition of O to furan and pyrrole at the ortho position.

The relatively high $\Delta G^{\ddagger}$ for the H-atom abstraction channel leads to rate constants that are 10^7-10^{10} times slower than for the addition channel at 298 K. The Arrhenius plots for the H-atom abstraction by O atom from all of the aromatic rings studied exhibit some curvature and are, therefore, better described by a plot of eq 13. Analogous to the reactions of these aromatic hydrocarbons with H atoms, the activation barriers (E_{0K}) for the H-atom abstraction channel are modest ($\leq$ 4.5 kcal mol^{-1}) for the six-membered rings, but are considerably higher ($\geq$ 10 kcal mol^{-1} in most cases) for the five-membered rings.

For the reaction of O atom with a heteroatomic aromatic ring, there is one experiment to which the B3LYP calculations can be compared. Lee and Tang[47] determined the absolute rate constant for the reaction of atomic oxygen with thiophene by measuring the depletion of O atom. At low temperatures, they observed a negative activation energy of −2.6 kcal mol^{-1}. Due to the nature of the experiment, they were not able to determine if the reaction proceeded by addition or abstraction or which site was the reacting center. The B3LYP calculations (Table 4) suggest that only the addition channel will be accessible. However, to make the best comparison with experiment, the sum of the calculated reaction rates for each channel at each unique site in thiophene was used. A fit of the subsequent ln k_{Total} vs $1/T$ plot gave an Arrhenius energy of −3.6 kcal mol^{-1}, which is in reasonably good agreement with the experiment (−2.6 kcal mol^{-1}).

The addition channel dominates the reaction mechanism of the O atom reactions with the five-membered rings even at the highest temperatures studied (Table 4). It is apparent that the abstraction pathway is preferred over the addition pathway at lower temperatures for six-membered rings as compared to five-membered rings.

Reactions of Hydroxyl Radical with Benzene. The B3LYP method was used to study the reaction of benzene with OH radicals for the addition channel to form the hydroxycyclohexadienyl radical $C_6H_6OH\bullet$ and the H-atom abstraction channel to form $C_6H_5\bullet + H_2O$. The thermodynamic results are quite different for the reaction of benzene with OH than for the previously presented reactions with H and O atoms. At room temperature, addition of OH radical ($\Delta G^{\ddagger} = 6.7$ kcal mol^{-1}) has a lower barrier than abstraction of a ring hydrogen atom ($\Delta G^{\ddagger} = 7.2$ kcal mol^{-1}). However, due solely to the inclusion of the Wigner tunneling correction factor, the B3LYP-TST method calculates kinetic rate constants that show a preference for abstraction of a ring hydrogen atom over addition of OH radical to benzene (Table 5). In either case, the B3LYP method calculates a rate constant at 298 K that is slower than that determined by experiment.[41-44,77]

Arrhenius plots for the calculated rate constants derived from the B3LYP energies for both the OH addition and H-atom abstraction channels are markedly nonlinear (Figure 3) over the entire temperature range studied, 250−2000 K. Therefore, it is not practical to compare the B3LYP Arrhenius activation barriers calculated over this temperature range with those from experiment. However, a fit to the linear plot of ln(k/T^m) vs $1/T$ for the OH addition pathway to benzene yields an E_{0K} that is lower (0.14 kcal mol^{-1}) than that for the corresponding H-atom abstraction channel. This is further evidence that the B3LYP-TST method is useful for identification of the most probable reaction channel.

Ravishankara and co-workers[42] have studied the reaction of hydroxyl radicals with benzene over an extended temperature range, 250−1000 K, by monitoring the extent of OH reaction. Although the temperature-dependent mechanism was found to be complicated, three major reaction channels that dominate the kinetics in distinct temperature regions have been identified by these authors and others. At T $\leq$ 298 K, the dominant channel

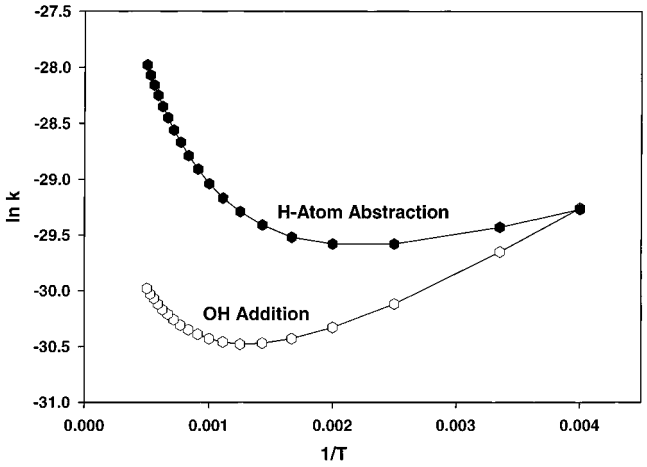

Figure 3. Arrhenius plot for the B3LYP-TST rate constants for the C_6H_6 + OH reaction through the temperature range of 250−2000 K. The OH addition channel is a low-temperature pathway shown with open hexagons. The H−atom abstraction channel is a high-temperature pathway shown with filled hexagons.

was the addition of OH to benzene to form the thermalized adduct C_6H_6OH•. Arrhenius fits to the low-temperature experiments gave an activation barrier for the addition reaction of 0.9[41] and 0.5[42] kcal mol^{-1}. If calculated rate constants are fit over the experimental temperature range at which OH addition was observed, the B3LYP-TST E_a is −1.2 kcal mol^{-1}.

Experimentally, decomposition of the C_6H_6OH• adduct back to reactants was observed at temperatures between 300 and 500 K. There is good agreement between experiments[41,43,77] that this decomposition reaction occurs with an activation barrier of ∼19 kcal mol^{-1}. The B3LYP-TST E_a for this reaction is 13.3 kcal mol^{-1} for the same temperature range. It has been observed that at T ≥ 500 K, the dominant reaction pathway becomes H-atom abstraction. Although there is some, albeit small, discrepancy in the experimental rate constants for the H-atom abstraction channel, there is a consensus that the activation barrier for the formation of C_6H_5• + H_2O is ∼4 kcal mol^{-1}.[41,42,44] The E_a determined by a fit of the B3LYP-TST rate constants for the temperature range 500−1500 K is 1.7 kcal mol^{-1}.

Reactions of Hydroxyl Radical with Heteroatomic Aromatic Hydrocarbons. A summary of the B3LYP calculated thermodynamic and kinetic parameters for the reaction of the monocyclic aromatic rings with hydroxyl radical is presented in Table 5. The transition state and reaction free energies for the addition of OH to pyridine are quite similar to those for addition of H and O atoms to each unique carbon site. It is noteworthy, however, that unlike the earlier H and O atom reactions, the reaction of hydroxyl radicals with pyridine for the H-atom abstraction channel is exoergic at 298 K. The $\Delta G^{\ddagger}$ for the abstraction channel is also lower than for the analogous reactions with H and O atom. Furthermore, the free energy barrier for the transition state for H-atom abstraction from the ortho and para positions of pyridine is lower than the corresponding barrier for OH addition.

In contrast, the dominant mechanism for reaction of OH radicals with the five-membered rings (furan, thiophene, and pyrrole) remains addition at room temperature (Table 6). In general, the activation barrier for addition of H, O, or OH to the five-membered aromatic rings is ∼2 kcal mol^{-1} lower than addition to the six-membered aromatic rings. A comparison of the $k_{add}/k_{abstract}$ ratio (Table 6) throughout the temperature range 298−2000 K indicates that H-atom abstraction from thiophene and pyrrole is only likely at elevated temperatures ($T \geq 1000$ K).

TABLE 6: A Comparison of $k_{add}/k_{abstract}$ as a Function of Temperature for the Reaction of Aromatic Hydrocarbons with OH radical[a,b]

		298 K	500 K	1000 K	1500 K	2000 K
benzene		0.45	0.27	0.14	0.10	0.076
pyridine	2	0.00008	0.0019	0.014	0.025	0.031
	3	0.48	0.35	0.21	0.15	0.13
	4	0.014	0.042	0.074	0.077	0.074
furan	3	8201	94	2.6	0.69	0.34
thiophene	2	6.6×10^4	402	7.1	1.6	0.73
	3	97	7.8	0.94	0.40	0.25
pyrrole	3	7200	89	2.6	0.71	0.35

[a] $k_{add}/k_{abstract}$ ratios were not calculated for furan and pyrrole at the 2 position due to the lack of a transition state barrier for either the OH addition or H-atom abstraction channel. [b] Rate constants were calculated using eq 9 based on the B3LYP/6-311+G(d,p)//B3LYP/6-31G(d) level of theory.

TABLE 7: Free Energies[a] (298 K) for the Transition Structures and Products of the Addition Reactions Ar + X → ArX (X = H, O (^{3}P), OH) at the B3LYP/6-311+G(d,p)// B3LYP/6-31G(d) Level of Theory

		H atom		O (^{3}P) atom		OH radical	
	site	TS	product	TS	product	TS	product
thiophene	2	7.6	−29.5	3.0	−20.9	4.0	−18.4
	3	9.0	−18.5	5.7	−8.8	6.4	−6.1
	S	*b*	2.6	*b*	2.8	*b*	4.0
pyrrole	2	6.3	−21.6	*c*	−19.4	*c*	−15.5
	3	8.9	−12.7	4.3	−6.3	5.4	−3.2
	N	23.7	21.4	37.0	37.1	*d*	*d*

[a] Energies are relative to reactants in kcal·mol^{-1}. [b] Transition structures were not obtained for this reaction. [c] Barrierless reaction. [d] Transition state and product do not exist for this reaction.

Reactions at S and N Heteroatoms. Addition of O and OH to the S and N heteroatoms in thiophene and pyrrole has been postulated as a mechanism by which thiophene and pyrrole undergo decomposition that is different from furan. This explanation was used to rationalize the different kinetic measurements for these compounds.[46−48,51,52,55] In general, the available experimental kinetic data do not distinguish between addition and abstraction pathways. Furthermore, the experiments have usually not discerned the mechanism for addition, i.e., to which unique carbon the radical is being added or whether the radical adds directly to the heteroatom.[1,46−48,52,55]

It is evident from the calculations presented in Table 7 that addition to the heteroatoms in pyrrole and thiophene is not a thermodynamically preferred pathway as compared to addition to ring carbon atoms. For example, addition of O (^{3}P) to the nitrogen atom in pyrrole is an endoergic step and is ∼40 kcal mol^{-1} less favorable than addition to the ortho carbon atom. Furthermore, the activation barrier for addition to the heteroatom is also at least 30 kcal mol^{-1} higher than that for the carbon atoms in pyrrole. Also, a minimum could not be found for the addition of OH radical directly to the nitrogen atom in pyrrole.

Similarly, it is not thermodynamically favorable for the reaction of thiophene with any of the small radicals studied to proceed via addition to the sulfur atom. Radical addition at the ring carbon atoms in thiophene is an exoergic process, yet addition to sulfur is an endoergic step. Furthermore, the H, O, and OH addition products to sulfur might better be described as the formation of a complex rather than a covalent bond. The bond distances between S−X are 3.5, 2.5, and 2.5 Å for X = H, O, and OH, respectively. The B3LYP calculations presented here apparently rule out a pathway for addition to the heteroatoms.

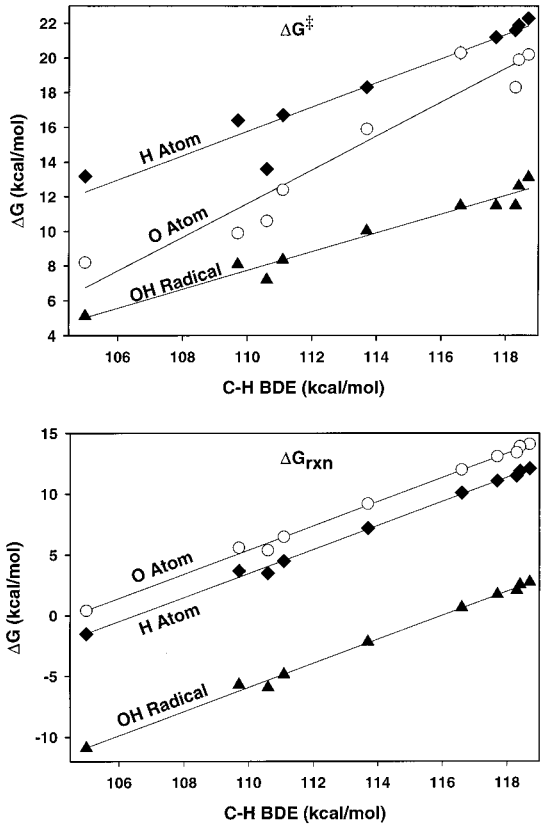

Figure 4. Correlation for the transition state (top) and reaction (bottom) free energies for H-atom abstraction from several aromatic hydrocarbons as a function of C−H BDE. The C−H BDEs are taken from ref 5.

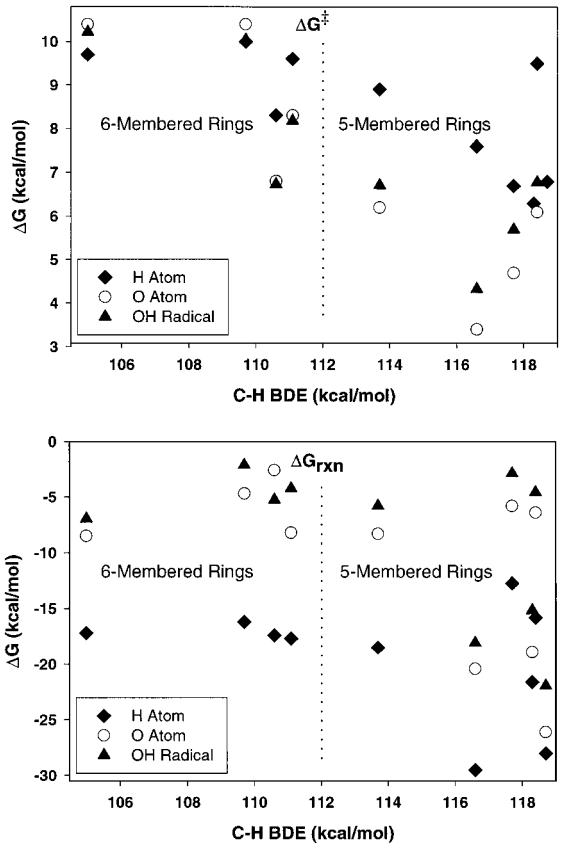

Figure 5. Correlation for the transition state (top) and reaction (bottom) free energies for radical addition to several aromatic hydrocarbons as a function of C−H BDE. The C−H BDEs are taken from ref 5.

Discussion

Relative Reactivity of Aromatic Hydrocarbons with H, O, and OH. Reaction with hydroxyl radical is the most exoergic reaction for all of the monocyclic aromatic rings, and the OH reaction also has the lowest barrier height. In general, Hammond's postulate is not obeyed for the reactions of aromatic hydrocarbons with hydrogen and oxygen atoms because the formation of OH radical via H-atom abstraction by O (^{3}P) is the least favorable process, although the activation barrier for abstraction by H-atom is most often the highest. This effect was noted earlier for the study of H and O reactions with methane by Schlegel and co-workers.[14] The temperature at which the abstraction channel becomes kinetically and thermodynamically preferred over the addition channel for the monocyclic aromatic rings increases in the order OH < O (^{3}P) < H.

Addition vs Abstraction for Monocyclic Aromatic Hydrocarbons. In general, the barrier to H-atom abstraction from five-membered rings is higher than that for six-membered rings. One source of this difference is that the C−H BDEs of the five-membered rings are greater than those in the six-membered rings.[5] A more general statement can be made that both the transition state and reaction free energies for the H-atom abstraction reactions from each unique carbon site are directly proportional to the relative C−H bond strengths, as illustrated in Figure 4. The $\Delta G^{\ddagger}$ dependence on the C−H BDE is significantly sharper for O (^{3}P) than for H and OH.

Furthermore, Hammond's postulate is obeyed and the barrier heights for H-atom abstraction by the same abstracting agent follows the order of the C−H BDEs. The progress along the reaction coordinate (as determined by the breaking C−H bond length in the transition state structure: 1.412, 1.484, and 1.591 Å for pyridine, benzene, and furan, respectively) is also consistent with the free energies for the abstraction reactions.

In general, the thermodynamically preferred site for addition is the site from which abstraction of a hydrogen atom requires the most energy, i.e., the site of the strongest C−H bond. Nevertheless, the transition state free energies for radical addition to the aromatic rings do not correlate well with the C−H BDEs (Figure 5). The overall reaction free energy (bottom trace, Figure 5) for the addition of H, O, and OH to the six-membered rings does appear to be relatively well correlated, whereas addition to the five-membered rings is not well correlated at all.

Cleavage of the C−H bonds leads to a σ aryl radical that is largely unaffected by the π system of the molecule. However, the addition of a radical to the aromatic system significantly disrupts the π system and creates a π aryl radical. As shown in Figure 6, there is a significant difference in resonance stabilization of the π radicals between the six- and five-membered rings. At all positions for addition to the ring, the six-membered ring π radicals have three resonance structures that make significant contributions to the overall electronic structure of the π radical. Thus, the electronic structure of the π radical does not suggest that one position will be more stable than another position for the six-membered rings. This is supported by the energetic results shown in Tables 1, 3, and 5.

However, there is a clear difference in positions for addition to the five-membered rings. Because addition at the ortho position to the heteroatom leads to a π radical with two resonance structures and addition to the meta position leads to a π radical with only one important resonance structure, addition to the ortho position will be significantly more favored, as is seen in Tables 1, 3, and 5. Because the energetics of the addition

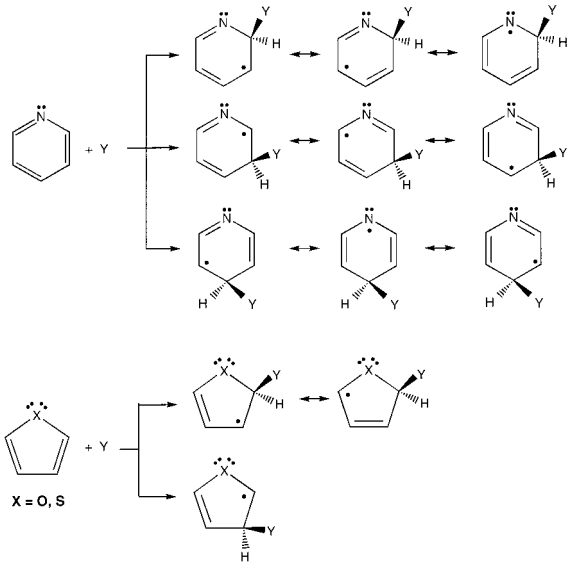

Figure 6. Resonance structures for radical addition to each unique site in heteroatomic five- and six-membered aromatic rings.

TABLE 8: Absolute Temperatures (K) at Which the Abstraction Barrier Becomes Lower than the Addition Barrier ($T_{T.S.}$) and the Abstraction Channel Becomes Thermodynamically Favored over the Addition Channel (T_{rxn})[a]

		H atom		O (^{3}P) atom		OH radical	
	site	T_{TS}	T_{rxn}	T_{TS}	T_{rxn}	T_{TS}	T_{rxn}
benzene	1	1155	1004	1065	528	245	259
pyridine	2	1830	833	*b*	781	*b*	166
	3	2710	1071	1155	966	*b*	264
	4	3910	963	265	841	*b*	173
furan	2	4190	1639	*c*	1673	*c*	987
	3	3090	1230	2150	1111	1325	496
thiophene	2	3615	1625	2730	1467	1770	821
	3	3070	1201	1850	1039	975	476
pyrrole	2	3350	1343	*c*	1407	*c*	759
	3	2985	1093	*c*	1115	1335	422

[a] B3LYP/6-311+G(d,p)//B3LYP/6-31G(d) level of theory. [b] Abstraction is kinetically preferred over addition at all temperatures. [c] Comparison could not be made because reaction was either barrierless or the transition state could not be located.

to the five-membered rings are dominated by the electronic structure of the π system, no correlation between the energies of the adducts and the C−H BDEs for generating σ aryl radicals is expected or observed.

Temperature Effects on Reaction Pathway. In general, the room-temperature barrier height for the addition channel is lower than that for the abstraction channel (Tables 1, 3, and 5). Several experiments have shown that the H-atom abstraction channel becomes the dominant pathway for benzene at high temperatures,[28,37,41,42,44] and these results have been supported by the B3LYP calculations. Because fewer experiments have been performed throughout an extended temperature range for the heteroatomic rings, it is also of interest to apply the same B3LYP-TST method to calculate the crossover temperature at which the H-atom abstraction channel will be preferred over the addition channel. A complete summary of the temperatures at which H-atom abstraction becomes kinetically (based on the crossover temperature for the Arrhenius plots) and thermodynamically (based on reaction free energy calculations) preferred over radical addition to the aromatic ring is given in Table 8.

In general, the crossover temperature at which H-atom abstraction becomes preferred over radical addition of the radical to the ring is well-correlated with the C−H BDE, i.e., the more stable the nascent aryl radical, the lower the crossover temperature will be. The crossover temperatures for OH radical reactions are lower than for H and O atom reactions. For example, for the C_6H_6 + OH reaction, the free energy barrier for the abstraction channel becomes lower than the barrier for the addition channel at a lower temperature (~245 K) than for the analogous reactions with hydrogen and oxygen atoms. These results are in good qualitative agreement with the temperature-dependent experimental studies of the reaction of OH with benzene.[41,42,44]

Comparison of B3LYP Thermochemical Calculations with Experiment for Aromatic Hydrocarbon Reactions. DFT methods, including the B3LYP method, have been invaluable at providing computational insight into problems in which the size of the system makes more expensive calculations prohibitive. For example, the B3LYP method can be used to quite accurately predict the C−H bond dissociation enthalpies (BDE) of the aromatic hydrocarbons relevant to combustion chemistry.[5]

There are no experimental data for the total energies for the initial reaction of benzene with H, O (^{3}P), and OH. However, the reaction enthalpy for the abstraction reactions can be estimated from the relevant BDEs (Table 9). The enlarged basis set (6-311+G(d,p)) used with the B3LYP method in this paper is a prerequisite for obtaining reliable energies. Yet, the error in the calculation of the HO−H BDE by the B3LYP method is still ~4 kcal mol^{-1}. Although the CBS-QB3 method[62] is a more accurate method to calculate the HO−H BDE, this composite method slightly overestimates the nonpolar H−H BDE. It is evident from Table 9 that the CBS-QB3 method has the lowest absolute error in the calculation of the four BDEs relevant to these calculations. In general, however, the CBS-QB3 method is far more expensive and therefore less desirable for application to the survey of aromatic systems presented in this paper. Table 9 also includes the same BDE calculated using the hybrid HF-DFT method MPW1K. This method was recently developed to reduce the error in reaction barrier heights over other widely used computational methods. However, the MPW1K method calculates BDEs that are both lower than the experimental BDEs and do not agree as well as the BDEs calculated by the B3LYP/6-311+G(d,p)//B3LYP/6-31G(d) method for the small subset of BDEs considered here.

A comparison of the reaction enthalpies for the H-atom abstraction from benzene by H, O (^{3}P), and OH can be seen in Table 10. The discrepancies between the experimental values and the B3LYP/6-311+G(d,p)//B3LYP/6-31G(d) calculated reaction enthalpy for the H and O atom processes can be almost wholly attributed to the difference between the calculated and experimental C−H bond for benzene, an issue that has been previously noted.[5,6] The H−H and O−H BDEs calculated at the B3LYP/6-311+G(d,p)//B3LYP/6-31G(d) level of theory are in very good agreement with the experimental values. However, reaction energies for OH abstraction reactions also differ from experiment because of the persistent underestimation of the calculated HO−H BDE.

Validity of the B3LYP-TST Method for Calculation of Kinetic Parameters of Aromatic Hydrocarbon Reactions. The kinetic parameters presented in Tables 1, 3, and 5 were fits to plots from T = 298−2000 K, a temperature range over which many of the Arrhenius plots are nonlinear. However, many of the experimental reactions of benzene with H, O, and OH have been studied over smaller temperature ranges. Therefore, to calculate E_a values that can be compared directly to experimental kinetic parameters, the Arrhenius parameters

TABLE 9: Bond Dissociation Enthalpies (at 298 K, in kcal mol^{-1})

ΔH_{298} (R−H)	expt	B3LYP /6-31G(d)	B3LYP/6-311+G(d,p) //B3LYP/6-31G(d)	CBS-QB3	MPW1K /6-31+G(d,p)
C_6H_5−H	113.5[a]	110.8	110.6	115.4	110.0
H−H	104.2[b]	104.4	104.6	105.3	100.7
O−H	102.2[b]	97.9	102.7	102.7	97.5
HO−H	119[b]	109.5	114.9	119.2	111.8

[a] Davico, G. E.; Bierbaum, V. M.; DePuy, C. H.; Ellison, G. B.; Squires, R. R. *J. Am. Chem. Soc.* **1995**, *117*, 2590−2599. [b] *CRC Handbook of Chemistry and Physics*; 69th ed.; Weast, R. C.; Astle, M. J.; Beyer, W. H., Eds.; CRC Press: Boca Raton, FA, 1988−1989.

TABLE 10: Reaction Enthalpies for H-Atom Abstraction Reactions (at 298 K, in kcal mol^{-1})

reaction	expt[a]	B3LYP/6-311+G(d,p)// B3LYP/6-31G(d)	MPW1K/ 6-31+G(d,p)
$C_6H_6 + H \rightarrow C_6H_5 + H_2$	+ 9.3	+ 6.0	+ 9.3
$C_6H_6 + O \rightarrow C_6H_5 + OH$	+ 11.3	+ 7.9	+ 12.5
$C_6H_6 + OH \rightarrow C_6H_5 + H_2O$	−5.5	−4.3	−1.8

[a] Reaction enthalpies were computed from experimental data in Table 9 by the expression [ΔH_{298} (C_6H_5−H) − ΔH_{298} (X−H)] where X = (H, O, or HO).

TABLE 11: Calculated B3LYP-TST and MPW1K-TST Arrhenius Activation Energies, E_a, (in kcal mol^{-1}) for Benzene Reactions[a]

reaction	T (K)	expt	B3LYP-TST	MPW1K-TST
$C_6H_6 + H \rightarrow C_6H_7$	300−400	3.3,[23] 4.3[24]	2.90 ± 0.01	3.8 ± 0.01
$C_6H_5 + H_2 \rightarrow C_6H_6 + H$	550−1025	9.7[22]	4.53 ± 0.09	5.53 ± 0.08
$C_6H_6 + O \rightarrow C_6H_6O$	700−1300	4.0,[33,36] 4.8,[31] 5.0[32]	0.65 ± 0.10	6.0 ± 0.10
$C_6H_6 + OH \rightarrow C_6H_6OH$	250−300	0.9[41], 0.5[42]	−1.20 ± 0.01	2.36 ± 0.01
$C_6H_6OH \rightarrow C_6H_6 + OH$	300−500	19[41,43,76]	13.29 ± 0.04	20.22 ± 0.04
$C_6H_6 + OH \rightarrow C_6H_5 + H_2O$	500−1500	4.0[41,42,44]	1.7 ± 0.4	7.0 ± 0.4

[a] Using rate constants derived from the B3LYP/6-311+G(d,p)//B3LYP/6-31G(d) and MPW1K/6-31+G(d,p) energies that are used with eq 12 for the temperature range indicated.

were recalculated by a fit over the experimental temperature range for which either radical addition or H-atom abstraction was observed. A summary of the B3LYP-TST, the MPW1K-TST, and the available experimental E_as for reactions with benzene are reported in Table 11.

It can be seen that the B3LYP-TST method consistently underestimates the E_a by ∼4 kcal mol^{-1}. The discrepancy is as great as ∼6 kcal mol^{-1} for the decomposition reaction $C_6H_6OH \rightarrow C_6H_6 + OH$, but as low as ∼1.5 kcal mol^{-1} for the addition reaction $C_6H_6 + H \rightarrow C_6H_7$. Although the B3LYP-TST method does not appear to be suitable for the calculation of absolute rate constants, it can be used to calculate E_a within a few kcal mol^{-1}. Furthermore, a comparison of the ratio of rate constants $k_{add}/k_{abstract}$ can reduce the errors that result from the B3LYP method by canceling errors inherent to the B3LYP geometries and energies. As a result, the B3LYP-TST method is useful for the purpose of deciding whether a reaction channel is significant (such as radical addition vs H-atom abstraction) at a particular temperature for the reaction of aromatic hydrocarbons with H, O, and OH. Furthermore, the B3LYP calculated crossover temperature at which H-atom abstraction becomes preferred over radical addition is in good agreement with experiment for all the cases studied here.

Implications for Combustion Chemistry. Although only the initial reactions of H, O, and OH with aromatic hydrocarbons have been explored in this work, the results of this study have significant implications for the final products of aromatic hydrocarbon combustion. The reaction of pyridine with O atom will be used to illustrate this statement. H-atom abstraction reactions will occur at either the ortho or para positions of pyridine to yield a pyridyl radical. Thermal decomposition of these pyridyl radicals has been shown to lead to products of either acetylene (C_2H_2), cyanoacetylene (NCCCH), and OH or hydrogen cyanide (HCN), diacetylene (HCCCCH), and OH.[78] The pyridine-O adduct formed by the addition of O atom to pyridine at the meta position is likely to undergo H-atom rearrangement followed by CO loss,[79] resulting in pyrrolenine, a rearranged form of pyrrole. The subsequent decomposition of pyrrolenine[80] has been shown to yield CO, HCN, and propyne ($HCCCH_3$). The B3LYP calculations show that the H-atom abstraction channel will be preferred at all temperature for reaction at the 2 and 4 positions and will be competitive at $T >$ 1000 K at the 3 position. Due to the thermodynamic preference for H-atom abstraction, the final products of the decomposition of the pyridyl radical will be C_2H_2, NCCCH, HCN, HCCCCH, and OH.

Conclusions

The initial reactions of H, O (^{3}P), and OH with monocyclic aromatic hydrocarbons have been studied using the B3LYP method and transition state theory. The calculated free energies and reaction rate constants suggest that the radical addition channel is preferred at 298 K, but the H-atom abstraction channel becomes dominant at high temperatures. The specific crossover temperature is very dependent upon the reacting radical and the aromatic ring. The thermodynamic preference for reactivity with aromatic hydrocarbons increases in the order O(^{3}P) < H < OH.

Abstraction from six-membered aromatic rings is more facile than abstraction from five-membered aromatic rings. In general, the barrier height and the site preference for abstraction from sites within the aromatic hydrocarbon are correlated with the corresponding C−H BDE, but there is no analogous correlation for the radical addition energies. However, radical addition to five-membered rings is kinetically preferred and thermodynamically more exoergic than radical addition to six-membered rings.

The subsequent reaction pathways available following the initial addition of H, O, and OH to aromatic hydrocarbons of

relevance to low-temperature atmospheric chemistry are the subject of a study that will be reported in a separate paper.[81] The oxidative decomposition of the aromatic radicals formed by the H-atom abstraction channel of relevance to high-temperature combustion chemistry has been the focus of several recent papers.[16,17,82−84]

During the review process, we became aware of a new hybrid HF-DFT method, the MPW1K formalism, which has been shown to improve the calculation of barrier heights for reactions involving smaller systems by a factor of 3 over the B3LYP method. To test if this technique would provide better agreement with experiment than the B3LYP method for the reactions studied in this paper, we employed the MPW1K/6-31+G(d,p) method to calculate the barriers for the radical addition and H-atom abstraction reactions of benzene. These results have been included in Tables 9−11. Our preliminary results indicate that the MPW1K-TST method yields E_a values that are ∼4.5 kcal mol^{-1} higher than the B3LYP-TST calculations and are on average higher than, but in better agreement with, the experimental barrier height. Further testing of this new method, which is currently underway in our group, is warranted to see if the MPW1K method is better suited to study the thermodynamic and kinetics of the reactions of aromatic hydrocarbons.

Acknowledgment. We gratefully acknowledge the U.S. Department of Energy (Grant DE-FG22-96PC96249) and the Ohio Supercomputer Center for support of this research. We also wish to thank George C. McBane (The Ohio State University) for helpful discussions on the kinetic formulation.

Supporting Information Available: Optimized geometries, energies, rotational constants, and vibrational frequencies. This material is available free of charge via the Internet at http://pubs.acs.org.

References and Notes

(1) Atkinson, R. *Chem. Rev.* **1985**, *85*, 69−201.
(2) Bittker, D. A. *Combust. Sci. and Technol.* **1991**, *79*, 49−72.
(3) Brezinsky, K. *Prog. Energy Combust. Sci.* **1986**, *12*, 1−24.
(4) Mebel, A. M.; Lin, M. C.; Yu, T.; Morokuma, K. *J. Phys. Chem. A* **1997**, *101*, 3189−3196.
(5) Barckholtz, C.; Barckholtz, T. A.; Hadad, C. M. *J. Am. Chem. Soc.* **1999**, *121*, 491−500.
(6) Cioslowski, J.; Liu, G.; Martinov, M.; Piskorz, P.; Moncrieff, D. *J. Am. Chem. Soc.* **1996**, *118*, 5261−5264.
(7) Cioslowski, J.; Liu, G.; Moncrieff, D. *J. Org. Chem.* **1996**, *61*, 4111−4114.
(8) Bauschlicher, C. W., Jr.; Langhoff, S. R. *Mol. Phys.* **1999**, *96*, 471−476.
(9) Parr, R. G.; Yang, W. *Density-Functional Theory of Atoms and Molecules*; Oxford University Press: New York, 1989.
(10) Labanowski, J. W.; Andzelm, J. *Density Functional Methods in Chemistry*; Springer: New Yorkl, 1991.
(11) Becke, A. D. *J. Chem. Phys.* **1993**, *98*, 5648−5652.
(12) Lee, C.; Yang, W.; Parr, R. G. *Phys. Rev. B* **1988**, *37*, 785−789.
(13) Hehre, W. J.; Radom, L.; Schleyer, P. v. R.; Pople, J. A. *Ab Initio Molecular Orbital Theory*; John Wiley & Sons: New York, 1986.
(14) Gonzalez, C.; McDouall, J. J. W.; Schlegel, H. B. *J. Phys. Chem.* **1990**, *94*, 7467−7471.
(15) Carpenter, B. K. *J. Am. Chem. Soc.* **1993**, *115*, 9806−9807.
(16) Barckholtz, C.; Fadden, M. J.; Hadad, C. M. *J. Phys. Chem. A* **1999**, *103*, 8108−8117.
(17) Fadden, M. J.; Barckholtz, C.; Hadad, C. M. *J. Phys. Chem. A* **2000**, *104*, 3004−3011.
(18) Liu, R.; Morokuma, K.; Mebel, A. M.; Lin, M. C. *J. Phys. Chem.* **1996**, *100*, 9314−9322.
(19) Kiefer, J. H.; Mizerka, L. J.; Patel, M. R.; Wei, H. C. *J. Phys. Chem.* **1985**, *89*, 2013−2019.
(20) Rao, V. S.; Skinner, G. B. *J. Phys. Chem.* **1984**, *88*, 5990−5995.
(21) Asaba, T.; Fujii, N. *Proc. 13th Int. Combust. Symp.* **1971**, 155−164.
(22) Park, J.; Dyakov, I. V.; Lin, M. C. *J. Phys. Chem. A* **1997**, *101*, 8839−8843.
(23) Sauer, M. C., Jr.; Ward, B. *J. Phys. Chem.* **1967**, *71*, 3971−3983.
(24) Sauer, M. C., Jr.; Mani, I. *J. Phys. Chem.* **1970**, *74*, 59−63.
(25) Yang, K. *J. Am. Chem. Soc.* **1962**, *84*, 3795.
(26) Knutti, R.; Buhler, R. E. *Chem. Phys.* **1975**, *7*, 229−243.
(27) Kim, P.; Lee, J. H.; Bonanno, R. J.; Timmons, R. B. *J. Chem. Phys.* **1973**, *59*, 4593−4601.
(28) Nicovich, J. M.; Ravishankara, A. R. *J. Phys. Chem.* **1984**, *88*, 2534−2541.
(29) Sibener, S. J.; Buss, R. J.; Casavecchia, P.; Hirooka, T.; Lee, Y. T. *J. Chem. Phys.* **1980**, *72*, 4341−4349.
(30) Bonanno, R. A.; Kim, P.; Lee, J. H.; Timmons, R. B. *J. Chem. Phys.* **1972**, *57*, 1377−1380.
(31) Nicovich, J. M.; Gump, C. A.; Ravishankara, A. R. *J. Phys. Chem.* **1982**, *86*, 1684−1690.
(32) Ko, T.; Adusei, G. Y.; Fontijn, A. *J. Phys. Chem.* **1991**, *95*, 8745−8748.
(33) Atkinson, R.; Pitts, J. N., Jr. *J. Phys. Chem.* **1975**, *79*, 295−297.
(34) Colussi, A. J.; Singleton, D. L.; Irwin, R. S.; Cvetanovic, R. J. *J. Phys. Chem.* **1975**, *79*, 1900−1903.
(35) Tabares, F. L.; Gonzalez Urena, A. *J. Phys. Chem.* **1983**, *87*, 4933−4936.
(36) Atkinson, R.; Pitts, J. N., Jr. *Chem. Phys. Lett.* **1979**, *63*, 485−489.
(37) Barry, N. J.; Fletcher, I. W.; Whitehead, J. C. *J. Phys. Chem.* **1986**, *90*, 4911−4912.
(38) Atkinson, R. *Atmos. Environ., A* **1990**, *24A*, 1−41.
(39) Atkinson, R. *J. Phys. Chem. Ref. Data* **1994**, *Monograph 2*, 1−216.
(40) Davis, D. D.; Bollinger, W.; Fischer, S. *J. Phys. Chem.* **1975**, *79*, 293−294.
(41) Perry, R. A.; Atkinson, R.; Pitts, J. N., Jr. *J. Phys. Chem.* **1977**, *81*, 296−304.
(42) Tully, F. P.; Ravishankara, A. R.; Thompson, R. L.; Nicovich, J. M.; Shah, R. C.; Kreutter, N. M.; Wine, P. H. *J. Phys. Chem.* **1981**, *85*, 2262−2269.
(43) Wahner, A.; Zetsch, C. *J. Phys. Chem.* **1983**, *87*, 4945−4951.
(44) Madronich, S.; Felder, W. *J. Phys. Chem.* **1985**, *89*, 3556−3561.
(45) Lin, C. Y.; Lin, M. C. *J. Phys. Chem.* **1986**, *90*, 425−431.
(46) Tabares, F. L.; Urena, A. G. *J. Chem. Soc., Faraday Trans. 2* **1985**, *81*, 1395−1405.
(47) Lee, J. H.; Tang, I. N. *J. Chem. Phys.* **1981**, *75*, 137−140.
(48) Gao, X.; Hall, M. P.; Smith, D. J.; Grice, R. *J. Phys. Chem. A* **1997**, *101*, 187−191.
(49) Schuler, R. H.; Laroff, G. P.; Fessenden, R. W. *J. Phys. Chem.* **1973**, *77*, 456−466.
(50) Samuni, A.; Neta, P. *J. Phys. Chem.* **1973**, *77*, 1629−1635.
(51) Lee, J. H.; Tang, I. N. *J. Chem. Phys.* **1982**, *77*, 4459−4463.
(52) Atkinson, R.; Aschmann, S. M.; Carter, W. P. L. *Int. J. Chem. Kinet.* **1983**, *15*, 51−61.
(53) Bierbach, A.; Barnes, I.; Becker, K. H. *Atmos. Environ.* **1992**, *26A*, 813−817.
(54) Bierbach, A.; Barnes, I.; Becker, K. H. *Atmos. Environ.* **1995**, *29*, 2651−2660.
(55) Wine, P. H.; Thompson, R. J. *Int. J. Chem. Kinet.* **1984**, *16*, 867−878.
(56) Frisch, M. J.; Trucks, G. W.; Schlegel, H. B.; Gill, P. M. W.; Johnson, B. G.; Robb, M. A.; Cheeseman, J. R.; Keith, T.; Petersson, G. A.; Montgomery, J. A.; Raghavachari, K.; Al-Laham, M. A.; Zakrzewski, V. G.; Ortiz, J. V.; Foresman, J. B.; Cioslowski, J.; Stefanov, B. B.; Nanayakkara, A.; Challacombe, M.; Peng, C. Y.; Ayala, P. Y.; Chen, W.; Wong, M. W.; Andres, J. L.; Replogle, E. S.; Gomperts, R.; Martin, R. L.; Fox, D. J.; Binkley, J. S.; Defrees, D. J.; Baker, J.; Stewart, J. J. P.; Head-Gordon, M.; Gonzalez, C.; Pople, J. A.; Gaussian 94, Revision C.3.; Gaussian, Inc.: Pittsburgh, PA, 1995.
(57) Scott, A. P.; Radom, L. *J. Phys. Chem.* **1996**, *100*, 16502−16513.
(58) Gonzalez, C.; Schlegel, H. B. *J. Chem. Phys.* **1989**, *90*, 2154−2161.
(59) Gonzalez, C.; Schlegel, H. B. *J. Phys. Chem.* **1990**, *94*, 5523−5527.
(60) Bacskay, G. B.; Martoprawiro, M.; Mackie, J. C. *Chem. Phys. Lett.* **1999**, *300*, 321−330.
(61) Wiberg, K. B.; Cheeseman, J. R.; Ochterski, J. W.; Frisch, M. J. *J. Am. Chem. Soc.* **1995**, *117*, 6535−6543.
(62) Montgomery, J.; Frisch, M.; Ochterski, J.; Petersson, G. *J. Chem. Phys.* **1999**, *110*, 2822−2827.
(63) Frisch, M. J.; Trucks, G. W.; Schlegel, H. B.; Scuseria, G. E.; Robb, M. A.; Cheeseman, J. R.; Zakrzewski, V. G.; Montgomery, J. A. J.; Stratmann, R. E.; Burant, J. C.; Dapprich, S.; Millam, J. M.; Daniels, A. D.; Kudin, K. N.; Strain, M. C.; Farkas, O.; Tomasi, J.; Barone, V.; Cossi, M.; Cammi, R.; Mennucci, B.; Pomelli, C.; Adamo, C.; Clifford, S.; Ochterski, J.; Petersson, G. A.; Ayala, P. Y.; Cui, Q.; Morokuma, K.; Malick, D. K.; Rabuck, A. D.; Raghavachari, K.; Foresman, J. B.; Cioslowski, J.;

Ortiz, J. V.; Stefanov, B. B.; Liu, G.; Liashenko, A.; Piskorz, P.; Komaromi, I.; Gomperts, R.; Martin, R. L.; Fox, D. J.; Keith, T.; Al-Laham, M. A.; Peng, C. Y.; Nanayakkara, A.; Gonzalez, C.; Challacombe, M.; Gill, P. M. W.; Johnson, B.; Chen, W.; Wong, M. W.; Andres, J. L.; Gonzalez, C.; Head-Gordon, M.; Replogle, E. S.; Pople, J. A.; Gaussian 98, Revision A.7.; Gaussian, Inc.: Pittsburgh, PA, 1998.

(64) Deegan, M. J. O.; Knowles, P. J. *Chem. Phys. Lett.* **1994**, *227*, 321−326.

(65) Hampel, C.; Peterson, K. A.; Werner, H.-J. *Chem. Phys. Lett.* **1992**, *190*, 1−12.

(66) Knowles, P. J.; Hampel, C.; Werner, H.-J. *J. Chem. Phys.* **1993**, *99*, 5219−5227.

(67) Purvis, G. D.; Bartlett, R. J. *J. Chem. Phys.* **1982**, *76*, 1910−1918.

(68) Lynch, B. J.; Fast, P. L.; Harris, M.; Truhlar, D. G. *J. Phys. Chem. A* **2000**, *104*, 4811−4815.

(69) Wigner, E. P. *Z. Phys. Chem.* **1932**, *B19*, 203.

(70) Noggle, J. H. *Physical Chemistry*; 1st ed.; Little, Brown and Company: Boston, 1985.

(71) Levine, I. N. *Physical Chemistry*; 4th ed.; McGraw-Hill: New York, 1995.

(72) Susnow, R. G.; Dean, A. M.; Green, W. H., Jr. *Chem. Phys. Lett.* **1999**, *312*, 262−268.

(73) Rice, B. M.; Pai, S. V.; Chabalowski, C. F. *J. Phys. Chem. A* **1998**, *102*, 6950−6956.

(74) Bach, R. D.; Glukhovstev, M. N.; Gonzalez, C.; Marquez, M.; Estevez, C. M.; Baboul, A. G.; Schegel, H. B. *J. Phys. Chem. A* **1997**, *101*, 6092−6100.

(75) Skokov, S.; Wheeler, R. A. *Chem. Phys. Lett.* **1997**, *271*, 251−258.

(76) Basch, H.; Hoz, S. *J. Phys. Chem. A* **1997**, *101*, 4416−4431.

(77) Lorenz, K.; Zellner, R. *Ber. Bunsen-Ges. Phys. Chem.* **1983**, *87*, 629−636.

(78) Hore, N. R.; Russell, D. K. *J. Chem. Soc., Perkin Trans. 2* **1998**, *2*, 269−276.

(79) Le Page, V.; Keheyan, Y.; Snow, T. P.; Bierbaum, V. M. *J. Am. Chem. Soc.* **1999**, *121*, 9435−9446.

(80) Martoprawiro, M.; Bacskay, G. B.; Mackie, J. C. *J. Phys. Chem. A* **1999**, *103*, 3923−3934.

(81) Barckholtz, C.; Hadad, C. M. *J. Phys. Chem. A*, to be submitted.

(82) Fadden, M. J.; Hadad, C. M. *J. Phys. Chem. A* **2000**, *104*, 6088−6094.

(83) Fadden, M. J.; Hadad, C. M. *J. Phys. Chem. A* **2000**, *104*, 6324−6331.

(84) Fadden, M. J.; Hadad, C. M. *J. Phys. Chem. A* **2000**, *104*, 8121−8130.